Towards a factored analysis of legged locomotion models

Richard Altendorfer,* Daniel E. Koditschek,* and Philip Holmes+

*Department of Electrical Engineering and Computer Science

The University of Michigan, Ann Arbor, MI 48109, USA;

+Department of Mechanical and Aerospace Engineering

Princeton University, Princeton, NJ 08544, USA.

Abstract

In this paper, we report on a new stability analysis for hybrid legged locomotion systems based on factorization of return maps. We apply this analysis to a family of models of the Spring Loaded Inverted Pendulum (SLIP) with different leg recirculation strategies. We obtain a necessary condition for the asymptotic stability of those models, which is formulated as an exact algebraic expression despite the non-integrability of the SLIP dynamics. We outline the application of this analysis to other models of legged locomotion and its importance for the stability of legged robots and animals.

1   Introduction

This paper introduces a new formalism for studying the stability of legged locomotion gaits and other periodic dynamically dexterous robotic tasks. We are most immediately motivated by the need to explain and control the remarkable performance of RHex, an autonomous hexapedal robot runner with unparalleled mobility [1]. Powered by only six actuators, located at the "hips" to drive each of its six passively compliant legs, RHex's locomotion is excited by a single periodic "clock" signal split into phase and anti-phase copies for coordinating its alternating tripod gait. A simple PD controller at each hip motor in a given tripod forces its leg to track the alternately fast and slow clock reference signal corresponding to putative stance and swing phases. Although RHex is currently being endowed with more sophisticated proprioceptive reflex loops to increase its responsiveness to varied terrain, we are strongly motivated to develop an analytical understanding of the relationship between clock signal and steady state gait properties in the "simple" open loop case.

A complete account of this relationship in even the simple case would entail insight into the steady state properties of an under-actuated high degree of freedom hybrid mechanical system whose Lagrangian dynamics switches between a set of 2^6 possible holonomically constrained models depending upon which toes are in contact with the ground. Fortunately, a growing body simulation study and empirical evidence [2] suggests that RHex, when properly tuned, exhibits sagittal plane stance behavior well approximated by the two degree of freedom SLIP. Thus, in the short term, we seek to understand how adjustments to a coordinating clock signal will determine the steady state performance of the bipedal SLIP underlying the alternating tripod gait. In this paper, we develop the mathematical foundations of a new formalism for distinguishing volume-preserving from non-volume-preserving hybrid Lagrangian systems. We apply this formalism to the hybrid SLIP model, the results of which suggest new insight into the relationship between clock excitation and steady state gait.

1.1   Leg Swing Policies and Self Stability in the SLIP Template

The SLIP model provides a ubiquitous description of biological runners in the sagittal plane [3] and, as mentioned above, a broadly useful prescription for legged robot runners such as RHex [4, 1, 2] as well. The closely related three degree of freedom Lateral Leg Spring (LLS), has been recently identified as a candidate template for cockroach running in the horizontal plane [5, 6] and seems likely to be relevant for RHex as well [1]. For present purposes, the most important insight from these models has been to provide a mathematical explanation for their unexpected "self-stability" properties (asymptotically stable equilibrium gaits in the absence of any sensor based feedback inputs), thus affording new hypotheses regarding biological control strategies [7] and a formal foundation for elucidating the stable open loop performance of RHex.

The originally discovered self-stability of SLIP [8, 9] is based on a simple leg swing policy, the leg touchdown angle at the end of aerial phases being kept constant from stride to stride. A similar strategy was earlier shown to yield stable gaits in the LLS model [6]. Recently, a different time-dependent leg retraction policy has been shown to inherit the stability properties of the fixed touchdown angle policy while increasing the robustness of the SLIP system [10]. On the other hand, numerical simulations of a recirculation policy where the SLIP's leg starts recirculating after leg liftoff at a constant angular velocity until leg touchdown suggest not asymptotic but neutral stability [11]. Hence the leg swing policy seems to play a central role in the stability of those low-dimensional models, as is also suggested by high dimensional systems such as RHex [1] or, as established in an independently conceived model inspired by animal locomotion strategies, for a quadrupedal trotter [12].

Stability of such systems is observed through the full-stride return map – the function relating body state at one stride to body state at next – which summarizes all properties relevant to the goal of translating the body center of mass. Unfortunately, even the simplest 2dof SLIP system is non-integrable [13], which precludes closed form solutions that might illuminate stability mechanisms. In this paper we will show how the stability of hybrid systems possessing certain symmetries can be analyzed in terms of their non-hybrid components, e.g. flight phase and stance phase in the case of SLIP, thus decomposing the hybrid return map into "partial" return maps that might be analyzed more easily.

Before doing so, we first introduce certain terminology and notation used throughout the paper by way of reviewing Liouville's theorem (see e.g. [14]), pointing out that the classical result should not be expected to apply in the present case.

1.2   Liouville's theorem and stability

Liouville's theorem states that volume in phase space of a holonomically constrained conservative dynamical system described by a single Hamiltonian flow is preserved, i.e. a set of initial conditions at $t = t_0$ in phase space will be mapped to a set with identical symplectic volume for any $t \geq t_0$.

In the case of non-holonomically constrained conservative Hamiltonian systems, the number of independent conjugate momenta is smaller than the number of independent configuration space variables and Liouville's theorem cannot be applied (see e.g. the asymptotic stability of the Chaplygin sleigh in [15] and references therein).

In the case of piecewise-defined holonomically constrained conservative Hamiltonian systems with different flows f_α^t with α in an indexing set I the transition to a new Hamiltonian flow is triggered by so-called threshold functions (for a general definition of hybrid systems see [16]). In almost all settings within robotics, these threshold functions between different flows f_α^t and f_β^t depend upon state, and often have no explicit time dependence at all. Examples include a discrete version of the Chaplygin sleigh [15, 17] and low-dimensional models of legged locomotion in the horizontal and sagittal plane [6, 8, 9], which all exhibit partial asymptotic stability for certain parameter settings. Here, the (local) asymptotic stability of those hybrid system at a fixed point means that the eigenvalues of the components of their linearized return maps defined by Poincaré sections lie within the unit circle (excluding those corresponding to conserved quantities). Liouville's theorem is not directly applicable due to the hybrid nature of such systems, despite the fact that the flows are Hamiltonian.

In those cases, the return map $\mathcal{R}$ defined by a Poincaré section is composed of several "factor" maps r_α^β that relate the state variables directly after one transition to those directly before the next. Additional transition mappings $\mathcal{T}_\alpha^\beta$ are used at transitions from flows f_α^t to f_β^t. They arise in practice from the fact that different flows are most easily handled analytically in different coordinate systems. Thus $\mathcal{R} = \mathcal{T}_\gamma^\alpha \circ r_\gamma^\alpha \circ \cdots \circ \mathcal{T}_\alpha^\beta \circ r_\alpha^\beta$.

1.3   Contribution of this paper

In this paper, we focus on the role of volume preservation in flows and transition maps of models of legged locomotion as an indicator of local stability. Although we cannot invoke Liouville's theorem for reasons just reviewed, we nevertheless deduce the necessity for volume preservation at a given fixed point in these flows, manifesting itself as the condition of unity determinant in the associated linearized return map. In general, in order to check whether the return map of a hybrid system $\mathcal{R}$ is volume-preserving at a fixed point, the map must be computed explicitly [17, 6, 8, 9]. However, we will show that if all vector fields f_α, $\alpha \in I$ possess time reversing symmetries $\mathcal{S}_\alpha$ and if the periodic orbit giving rise to a fixed point of $\mathcal{R}$ is composed of pseudosymmetric orbits (to be defined below) on each flow domain V_α, volume-preservation of the whole system can be determined by volume-preservation on individual flow domains. Moreover, if the transition function, h_α^β, from a flow domain, V_α, to a next flow domain, V_β, enjoys a certain symmetry related to the vector field's time reversing symmetry $\mathcal{S}_\alpha$, then volume preservation on V_α can be determined in certain cases without an explicit expression for the flow map

on that domain.

This paper introduces the rigorous foundations for the formalism just outlined, and provides an example of its value for robotics by application to the LLS [6] and SLIP [8, 9] models. As explained above, the question of whether a hybrid system is volume preserving or not has immediate consequences for gait stability. Since our conditions for volume preservation of the full stride return map may be checked with respect to a simple "factor map", we are able to study the effects of a broad range of leg swing policies that are implementable in the analytically tractable "flight" phase of the leg. Specifically, we show how the volume preserving properties of SLIP under different leg recirculation strategies can be determined by simple differentiation. In particular, in Sec.3.1.3 we give for the first time necessary conditions for asymptotic and neutral stability of a RHex-like leg recirculation scheme applied to the SLIP model, without explicit computation of the stance phase flow map.

2 Factoring return maps with time reversing symmetries

Assume a hybrid mechanical system whose time evolution is described by holonomically constrained autonomous conservative vector fields f_α, $\alpha \in I$ with configuration space variables q_α: $\dot{x}_\alpha = f_\alpha(x_\alpha)$ with $x = (q_\alpha \ \dot{q}_\alpha)^\top \in V_\alpha$. The open flow domains V_α are called charts [16]. Transitions between vector fields are governed by threshold functions h_α^β which can depend on the initial condition $x_{\alpha 0} = x_\alpha(t = 0) \in V_\alpha$, time t, and the current state $f_\alpha^t(x_{\alpha 0})$.[1] We demand that for each chart there is only one threshold function h_α^β. Transitions to the vector field f_β are uniquely defined by $t_{\alpha 0}^\beta(x_{\alpha 0}) = \min_{t>0}\{t : h_\alpha^\beta(f_\alpha^t(x_{\alpha 0}), x_{\alpha 0}, t) = 0\}$. In addition, all transition mappings $\mathcal{T}_\alpha^\beta$ are assumed to be volume preserving. The *flow map* r_α^β for the αth vectorfield is implicitly defined via $t_{\alpha 0}^\beta$ by $r_\alpha^\beta : x_{\alpha 0} \mapsto f_\alpha^{t_{\alpha 0}^\beta}(x_{\alpha 0})$, where $x_{\alpha 0}$ is assumed to be the result of a preceding chart transition.

We will define a partial return map for evolutions on individual charts V_α. Under the assumption that a periodic orbit of the whole dynamical system is composed of pseudo-symmetric orbits (to be defined below) on individual charts, volume preservation of the full return map $\mathcal{R}$ can be determined in some cases without explicitly computing r_α^β.

Assume that the vector field f_α admits a linear in-

volutive time reversing symmetry[2] $\mathcal{S}_\alpha$ ($-\mathcal{S}_\alpha \cdot \dot{x}_\alpha = f_\alpha(\mathcal{S}_\alpha \cdot x_\alpha) \Leftrightarrow \dot{x}_\alpha = f_\alpha(x_\alpha)$) with $\mathcal{S}_\alpha^2 = id$. This implies $\mathcal{S}_\alpha \circ f_\alpha^t \circ \mathcal{S}_\alpha = f_\alpha^{-t}$. We now investigate a composition of two *partial return maps*, $x_{\alpha 1} = \mathcal{S}_\alpha \circ r_\alpha^\beta(x_{\alpha 0})$, followed by $x_{\alpha 2} = \mathcal{S}_\alpha \circ r_\alpha^\beta(x_{\alpha 1})$. If the functional identity $t_{\alpha 1}^\beta = t_{\alpha 0}^\beta$ holds, then

$$\mathcal{S}_\alpha \circ r_\alpha^\beta \circ \mathcal{S}_\alpha \circ r_\alpha^\beta = \mathcal{S}_\alpha \circ f_\alpha^{t_{\alpha 0}^\beta} \circ \mathcal{S}_\alpha \circ f_\alpha^{t_{\alpha 0}^\beta} =$$
$$f_\alpha^{-t_{\alpha 0}^\beta} \circ f_\alpha^{t_{\alpha 0}^\beta} = id \quad (1)$$

We now need a sufficient condition for $t_{\alpha 1}^\beta = t_{\alpha 0}^\beta$. This is given by

$$\Big(h_\alpha^\beta(f_\alpha^{t_{\alpha 0}^\beta}(x_{\alpha 1}), x_{\alpha 1}, t_{\alpha 0}^\beta) = 0 \Leftrightarrow$$
$$h_\alpha^\beta(f_\alpha^{t_{\alpha 0}^\beta}(x_{\alpha 0}), x_{\alpha 0}, t_{\alpha 0}^\beta) = 0\Big) \Rightarrow t_{\alpha 1}^\beta = t_{\alpha 0}^\beta \quad (2)$$

which can be rewritten as

$$\Big(h_\alpha^\beta(f_\alpha^{t_{\alpha 0}^\beta} \circ S_\alpha \circ f_\alpha^{t_{\alpha 0}^\beta}(x_{\alpha 0}), S_\alpha \circ f_\alpha^{t_{\alpha 0}^\beta}(x_{\alpha 0}), t_{\alpha 0}^\beta) =$$
$$h_\alpha^\beta(S_\alpha(x_{\alpha 0}), S_\alpha \circ f_\alpha^{t_{\alpha 0}^\beta}(x_{\alpha 0}), t_{\alpha 0}^\beta) = 0\Big)$$
$$\Leftrightarrow \Big(h_\alpha^\beta(f_\alpha^{t_{\alpha 0}^\beta}(x_{\alpha 0}), x_{\alpha 0}, t_{\alpha 0}^\beta) = 0\Big) \quad (3)$$

which can be considered an invariance of the threshold function under the partial return map $\mathcal{S}_\alpha \circ r_\alpha^\beta : x_{\alpha 0} \mapsto S_\alpha \circ r_\alpha^\beta(x_{\alpha 0})$. This essentially checks that r_α^β is "compatible" with time reversibility of f_α.

Given that

$$\mathcal{S}_\alpha \circ r_\alpha^\beta \circ \mathcal{S}_\alpha \circ r_\alpha^\beta = id \quad (4)$$

then

$$D(\mathcal{S}_\alpha \circ r_\alpha^\beta \circ \mathcal{S}_\alpha \circ r_\alpha^\beta) =$$
$$D\mathcal{S}_\alpha \cdot Dr_\alpha^\beta(\mathcal{S}_\alpha \circ r_\alpha^\beta) \cdot D\mathcal{S}_\alpha \cdot Dr_\alpha^\beta = \mathbf{1} \quad (5)$$

Next, we call a trajectory on a chart V_α *pseudosymmetric* if a fixed point $\bar{x}_\alpha$ of the partial return map $\mathcal{S}_\alpha \circ r_\alpha^\beta$ with $\mathcal{S}_\alpha \circ r_\alpha^\beta(\bar{x}_\alpha) = \bar{x}_\alpha$ exists. Evaluation of expression (5) at such a fixed point then allows us to determine the square of the determinant of the Jacobian of r_α^β:

$$D\mathcal{S}_\alpha \cdot Dr_\alpha^\beta(\bar{x}_\alpha) \cdot D\mathcal{S}_\alpha \cdot Dr_\alpha^\beta(\bar{x}_\alpha) = \mathbf{1}$$
$$\det(D\mathcal{S}_\alpha \cdot Dr_\alpha^\beta(\bar{x}_\alpha) \cdot D\mathcal{S}_\alpha \cdot Dr_\alpha^\beta(\bar{x}_\alpha)) = 1$$
$$\det{}^2(Dr_\alpha^\beta(\bar{x}_\alpha)) = 1 \ .$$

Here $\det^2(D\mathcal{S}_\alpha) = 1$. Hence if a periodic orbit described by a fixed point of the full return map $\mathcal{R}$ is composed of pseudosymmetric orbits on V_α and conditions (2) hold on each chart, the full return map $\mathcal{R}$

---

[1]Note that this definition generalizes [16], where h_α^β only depends on $f_\alpha^t(x_{\alpha 0})$.

[2]The importance of time reversing symmetries for the asymptotic behavior of dynamical systems has been emphasized in [18].

is volume-preserving at this fixed point. If conditions (2) do not hold or if periodic orbits of the full return map are not composed of pseudosymmetric orbits, no conclusions can be drawn from this argument. Note that here "volume" is defined with respect to the state variables chosen, and in general is not a phase space volume, and that the computation (at the fixed point) is local.

3 Application to hybrid models of legged locomotion

3.1 SLIP with pitching

The SLIP model consists of a rigid body of mass m and moment of inertia I with a massless springy leg attached to an unactuated hip joint which is a distance d away from the center of mass (for details see [9]). A full stride consists of a stance phase with the foothold fixed and the leg under compression, and a flight phase in which the body describes a ballistic trajectory. Hence there are two vector fields f_1 (for stance) and f_2 (for flight) and the return map can be written as $\mathcal{R} = \mathcal{T}_2^1 \circ r_2^1 \circ \mathcal{T}_1^2 \circ r_1^2$. We assume that a periodic orbit of period one is composed of pseudosymmetric stance and flight phases.[3]

3.1.1 Stance phase of SLIP with pitching

The equations of motion that describe the stance phase of SLIP with mass m and moment of inertia I read in the conventions of Fig. 1 (see also [9]):

$$
\begin{aligned}
\ddot{\zeta} &= \zeta\dot{\psi}^2 - g\cos\psi - \frac{\partial_\eta V(\eta)}{m\eta}\left(\zeta + d\cos\left(\psi + \theta\right)\right) \\
\zeta\ddot{\psi} &= -2\dot{\zeta}\dot{\psi} + g\sin\psi + d\frac{\partial_\eta V(\eta)}{m\eta}\left(\sin\left(\psi + \theta\right)\right) \\
\ddot{\theta} &= d\zeta\frac{\partial_\eta V(\eta)}{\eta I}\sin\left(\psi + \theta\right)
\end{aligned} \tag{6}
$$

with spring potential $V(\eta)$ where the compressed spring length $\eta = \sqrt{d^2 + \zeta^2 + 2d\zeta\cos\left(\psi + \theta\right)} \leq \eta_0$, the relaxed spring length being denoted by η_0. The distance between the 'hip' pivot and the mass center is d and all joints, including the toe-ground pivot, are assumed frictionless and moment-free.

The linear involutive time reversing symmetry $\mathcal{S}_1$ of (6) acting on $x_1 = (\zeta\ \psi\ \theta\ \dot{\zeta}\ \dot{\psi}\ \dot{\theta})^\top$ is given by

$$
\mathcal{S}_1 = \mathrm{diag}(1, -1, -1, -1, 1, 1) . \tag{7}
$$

---

[3]This was proven in [9] for SLIP without pitching dynamics and without gravity in stance.
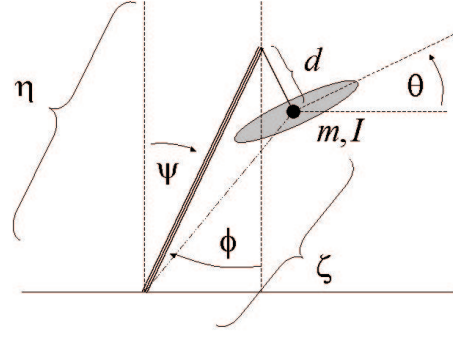
Figure 1: Parametrization of SLIP with pitching dynamics.

Under $\mathcal{S}_1$, the spring length η transforms as $\mathcal{S}_1(\eta) = \eta$. Transitions to flight occur when the spring length has reached its rest length η_0 which is also the initial spring length at the beginning of stance. Hence the threshold function can be written as $h_1^2(x_1(t), x_{10}, t) = \eta^2(t) - \eta_0^2$. Then the partial return map $\mathcal{S}_1 \circ r_1^2$ is volume-preserving at a fixed point, because (3) holds:

$$
\begin{aligned}
h_1^2(x_1(t_{10}^2), x_{10}, t_{10}^2) = \eta^2(t_{10}^2) - \eta_0^2 &= 0 \\
\Leftrightarrow h_1^2(\mathcal{S}_1 \cdot x_{10}, \mathcal{S}_1 \cdot x_1(t_{10}^2), t_{10}^2) = \eta_0^2 - \eta^2(t_{10}^2) &= 0
\end{aligned}
$$

This result is independent of the specific form of the spring potential $V(\eta)$. For $d = 0$, the two-dimensional SLIP system describing a point mass on a massless spring is recovered.

3.1.2 Flight phase of SLIP with pitching

The equation of motion of the center of mass that describe the flight phase of SLIP read

$$
\begin{aligned}
\ddot{y} &= 0 \\
\ddot{z} &= -g \\
\ddot{\theta} &= 0
\end{aligned} \tag{8}
$$

where the z-axis points vertically upwards, the y-axis points in a horizontal direction, and θ denotes the SLIP body's pitching angle with respect to the horizontal. The linear involutive time reversing symmetry $\mathcal{S}_2$ of (8) acting on $x_2 = (y\ z\ \theta\ \dot{y}\ \dot{z}\ \dot{\theta})^\top$ is given by

$$
\mathcal{S}_2 = \mathrm{diag}(\pm 1, 1, -1, \mp 1, -1, 1) . \tag{9}
$$

Here, the sign ambiguity in θ was resolved by matching θ's transformation to that of the stance phase (7). The transformation law of y under $\mathcal{S}_2$ is not needed in subsequent calculations and is left unresolved.

The simplicity of the equations of motion (8) allows us to explicitly compute the determinant of the Jacobian

of the partial return map $\mathcal{S}_2 \circ r_2^1$ at a fixed point for a given leg recirculation scheme. Therefore the application of the formalism of Sec. 2, which only provides a sufficient condition for volume-preservation, but not for non-preservation, is relegated to the appendix.

The equations of motion for the z and θ coordinates can be explicitly solved and read in dimensionless variables:

$$
\begin{aligned}
\tilde{z}(\tilde{t}) &= \tilde{z}_0 + \dot{\tilde{z}}_0 \tilde{t} - \frac{\tilde{t}^2}{2} \\
\dot{\tilde{z}}(\tilde{t}) &= \dot{\tilde{z}}_0 - \tilde{t} \\
\tilde{\theta}(\tilde{t}) &= \tilde{\theta}_0 + \dot{\tilde{\theta}}_0 \tilde{t} \\
\dot{\tilde{\theta}}(\tilde{t}) &= \dot{\tilde{\theta}}_0
\end{aligned} \tag{10}
$$

with $\tilde{t} = t\sqrt{\frac{g}{\eta_0}}$, $\tilde{z} = \frac{z}{\eta_0}$, $\dot{\tilde{z}} = \frac{\dot{z}}{\sqrt{\eta_0 g}}$, $\tilde{\theta}_0 = \theta_0$, and $\dot{\tilde{\theta}} = \dot{\theta}\sqrt{\frac{\eta_0}{g}}$. We now want to explore different strategies to position the leg during flight. Since the leg is assumed massless, any leg angle trajectory $\phi(\tilde{t})$ where ϕ is defined in Fig. 1 can be commanded.

The threshold function h_2^1 for a recirculating leg reads in dimensionless variables

$$
h_2^1(\tilde{x}_2(\tilde{t}), \tilde{x}_{20}, \tilde{t}) = \tilde{z}(\tilde{t}) + \tilde{d}\cos(\tilde{\theta}(\tilde{t})) - \cos(\phi(\tilde{t})) \tag{11}
$$

where $\tilde{d} = \frac{d}{\eta_0}$. Setting eq. (11) to zero determines the time from leg liftoff ($\tilde{t}_{LO} = 0$) to leg touchdown $\tilde{t}_{TD} := \tilde{t}_{20}^1$, for which in general a closed form solution does not exist. Then the flow map r_2^1 takes the dimensionless state vector $\tilde{x}_2 = (\tilde{z} \ \tilde{\theta} \ \dot{\tilde{z}} \ \dot{\tilde{\theta}})^\top$ (y and $\dot{y}$ are omitted) from its value at leg liftoff to that at touchdown: $r_2^1(\tilde{x}_{20}) = \tilde{x}_2(\tilde{t}_{TD})$. A fixed point of a pseudosymmetric flight trajectory satisfies $\tilde{x}_2 = \mathcal{S}_2 \circ r_2^1(\tilde{x}_2)$.

The determinant of the Jacobian of r_2^1 can easily be computed from the flight trajectory expressions (10), bearing in mind that the flight time $\tilde{t}_{TD}$ also depends on the initial conditions:

$$
\det(Dr_2^1) = 1 - \partial_{\dot{\tilde{z}}_0}\tilde{t}_{TD} + \dot{\tilde{z}}_0\partial_{\tilde{z}_0}\tilde{t}_{TD} + \dot{\tilde{\theta}}_0\partial_{\tilde{\theta}_0}\tilde{t}_{TD} \tag{12}
$$

In this expression, the leading term 1 is a consequence of Liouville's theorem, because $\tilde{z}$ and $\dot{\tilde{z}}$ and $\tilde{\theta}$ and $\dot{\tilde{\theta}}$ are canonically conjugate up to a trivial rescaling, whereas the remaining terms make the non-applicability of Liouville's theorem to this hybrid system with a state-dependent threshold function (11) explicit. Albeit $\tilde{t}_{TD}$ cannot be computed explicitly in general, $\tilde{t}_{TD} = 2\dot{\tilde{z}}_0$ at a fixed point of $\mathcal{S}_2 \circ r_2^1$ and $\cos(\phi(\tilde{t}_{TD})) = \tilde{z}_0 + \tilde{d}\cos(\tilde{\theta}_0), \sin(\phi(\tilde{t}_{TD})) = -\sqrt{1 - (\tilde{z}_0 + \tilde{d}\cos(\tilde{\theta}_0))^2}$ and $\theta(\tilde{t}_{TD}) = -\tilde{\theta}_0$. Hence using implicit differentiation of (11) the determinant at this fixed point can be written

in terms of partial derivatives of $\phi(\tilde{t})$

$$
\det\left(Dr_2^1(\bar{\tilde{x}}_2)\right) = 1 + \frac{\Delta_2^{1\,\mathrm{num}}}{\Delta_2^{1\,\mathrm{den}}} \tag{13}
$$

with

$$
\begin{aligned}
\Delta_2^{1\,\mathrm{num}} &= \sqrt{1 - (\tilde{z}_0 + \tilde{d}\cos(\tilde{\theta}_0))^2} \cdot \\
&\quad \left(-\partial_{\dot{\tilde{z}}_0}\phi(\tilde{t}_{TD}) + \dot{\tilde{z}}_0\partial_{\tilde{z}_0}\phi(\tilde{t}_{TD}) + \dot{\tilde{\theta}}_0\partial_{\tilde{\theta}_0}\phi(\tilde{t}_{TD})\right) \\
&\quad + \dot{\tilde{z}}_0 - \tilde{d}\sin(\tilde{\theta}_0)\dot{\tilde{\theta}}_0 \\
\Delta_2^{1\,\mathrm{den}} &= -\sqrt{1 - (\tilde{z}_0 + \tilde{d}\cos(\tilde{\theta}_0))^2}\partial_{\tilde{t}}\phi(\tilde{t}_{TD}) \\
&\quad - \dot{\tilde{z}}_0 + \tilde{d}\sin(\tilde{\theta}_0)\dot{\tilde{\theta}}_0
\end{aligned}
$$

The eigenvalues of the partial return map $\mathcal{S}_2 \circ r_2^1$ are $\lambda_1 = 1$ (vertical energy), $\lambda_2 = 1$ (rotational energy), $\lambda_3 = -1$, and $\lambda_4 = -\det(Dr_2^1(\bar{\tilde{x}}_2))$. It must be emphasized, however, that the eigenvalues of this partial return map are not equal to the eigenvalues of the total return map $\mathcal{R}$ at the fixed point. In particular, the eigenvalues of $\mathcal{R}$ can be complex, as in Fig. 2, below. Setting eq. (13) to 1 yields a partial differential equation for leg recirculation schemes $\phi(\tilde{t})$ that are volume preserving. In the following, for simplicity, we apply formula (13) to different leg recirculation schemes for SLIP without pitching dynamics, i.e. $\tilde{d} = 0$ and no $\tilde{\theta}$ dependence. The investigation of leg recirculation strategies of SLIP with pitching dynamics will be published elsewhere. For SLIP without pitching, the determinant at the fixed point simplifies to

$$
\begin{aligned}
\det(Dr_2^1(\bar{\tilde{x}}_2)) &= 1 + \\
&\frac{\sqrt{1 - \tilde{z}_0^2}\left(-\partial_{\dot{\tilde{z}}_0}\phi(\tilde{t}_{TD}) + \dot{\tilde{z}}_0\partial_{\tilde{z}_0}\phi(\tilde{t}_{TD})\right) + \dot{\tilde{z}}_0}{-\sqrt{1 - \tilde{z}_0^2}\partial_{\tilde{t}}\phi(\tilde{t}_{TD}) - \dot{\tilde{z}}_0}
\end{aligned} \tag{14}
$$

3.1.3 Analysis of Recirculation Strategies

Consider now the following family of leg recirculation schemes

$$
\begin{aligned}
\phi(\tilde{t}) &= k\arccos(\tilde{z}_0) + \alpha(\tilde{t} - l\dot{\tilde{z}}_0) \quad : k, l > 0 \\
&\text{with } \alpha(x) = 0 \text{ for } x < 0
\end{aligned} \tag{15}
$$

$k = 1$ means that recirculation starts at the leg liftoff angle; if $l = 1$, a certain angular trajectory is specified starting at apex (see the leg retraction scheme in [10]). The application of the partial return map $\mathcal{S}_2 \circ r_2^1$ on $\tilde{x}_{20}$ in the threshold function h_2^1 (3) in order to determine for which parameters of the leg recirculation schemes (15) volume is preserved is relegated to the appendix. Instead we proceed by explicitly computing $\det(Dr_2^1(\bar{\tilde{x}}_2))$. With the angular trajectory (15), the

determinant becomes

$$\det(Dr_2^1(\bar{x}_2)) = 1 + \frac{-l\sqrt{1-\tilde{z}_0^2}\dot{\alpha}(\dot{\tilde{z}}_0(2-l)) + \dot{\tilde{z}}_0(k-1)}{\sqrt{1-\tilde{z}_0^2}\dot{\alpha}(\dot{\tilde{z}}_0(2-l)) + \dot{\tilde{z}}_0} \quad (16)$$

Hence for different leg angle protocols we obtain

1. Constant leg touchdown angle protocol: $k = l = 0$, $\alpha = 2\pi - \beta \Rightarrow \det(Dr_2^1(\bar{x}_2)) = 0$. The two-dimensional Jacobian has rank one, and the return map becomes one-dimensional. In [8] this return map was parametrized by apex height, whereas in [9] the angle of the touchdown velocity was chosen. No information about the behavior of this lower-dimensional return map can be obtained from this argument.

2. Leg retraction [10]: $k = 0$, $l = 1$, and $\alpha(\tilde{t} - \dot{\tilde{z}}_0) = \alpha_A + \tilde{\omega}(\tilde{t} - \dot{\tilde{z}}_0)$ where α_A is a constant angle and $\tilde{\omega} = \omega\sqrt{\frac{\eta_0}{g}}$ is a constant dimensionless angular velocity. Then again $\det(Dr_2^1(\bar{x}_2)) = 0$ and the behavior of the remaining one-dimensional return map cannot be determined from this argument.

3. Leg recirculation (starting at leg liftoff): $l = 0$, $k > 0$, and $\alpha(\tilde{t}) = \alpha_A + \tilde{\omega}\tilde{t}$. This exemplifies the fast rotation phase of the open loop policy used by RHex [1], although a full analysis is beyond the scope of the present paper. Then for $\dot{\tilde{z}}_0 \geq 0$ and $\tilde{z}_0 \leq 1$ (necessary conditions for a pseudosymmetric flight phase):

$$\begin{aligned} \det(Dr_2^1(\bar{x}_2)) &= 1 - \frac{\dot{\tilde{z}}_0(1-k)}{\dot{\tilde{z}}_0 + \tilde{\omega}\sqrt{1-\tilde{z}_0^2}} \quad (17) \\ &= \begin{cases} < 1 & : \quad 0 < k < 1 \\ 1 & : \quad k = 1 \\ > 1 & : \quad k > 1 \end{cases} \end{aligned}$$

In order to illustrate the predictive power of eq. (17), we numerically approximate the determinant $\det(D\mathcal{R}(\bar{x}))$ of the full return map for fixed SLIP parameters $\tilde{E} = \frac{E}{mg\eta_0} = 2.1$, $\gamma = \frac{\kappa\eta_0}{mg} = 13$, and fixed recirculation parameters $\alpha_A = \pi$, $\tilde{\omega} = 14$ for different $k \in \{1/6, 0.5, 1, 2, 3.3\}$. Here, E is the total energy of the system and the spring potential is $V(\eta) = (\kappa/2)(\eta - \eta_0)^2$. We then compare these values to the values of the determinant obtained by inserting the numerically determined fixed points $\bar{x}_2 = (\bar{z}_0 \ \dot{\bar{z}}_0)^\top$ into eq. (17). The determinants obtained in those two different ways are plotted in Fig. 2a and agree to a high precision ($|\det(D\mathcal{R}(\bar{x})) - \det(Dr_2^1(\bar{x}_2))| < 10^{-7}$). Barring an improbable numerical cancellation between stance and flight phase dynamics, this also demonstrates that the SLIP's stance phase is volume pre-

serving.[4] In Figs. 2b-d iterations of the return map in $(\bar{z}_0 \ \dot{\bar{z}}_0)$-space are shown for $k \in \{1/6, 1, 3.3\}$ and initial conditions off the fixed point. The eigenvalues are complex conjugate pairs in all three cases. For $k = 1/6$ the trajectory spirals towards the fixed point, as expected from a stable fixed point (Fig. 2c), for $k = 1$ the trajectory is a deformed circle around the fixed point,[5] indicating neutral stability (Fig. 2d), and for $k = 3.3$ the trajectory spirals away from the fixed point, indicating instability (Fig. 2b).

3.2 Lateral leg-spring model

The lateral leg-spring (LLS) was introduced in [6]. We focus here on the three-degree-of-freedom version with pairs of 'virtual' elastic legs in intermittent contact with the ground. A full stride consists of two stance phases: a phase where the first elastic leg pivots around a "foothold" on one side of the rigid body, followed by a phase where the second elastic leg pivots around a "foothold" on the opposite side. See [6] for details. The equations of motion of both stance phases can be cast into the form (6) (with $g = 0$). Hence the stance phases from leg touchdown to liftoff are volume preserving. They are related by a transition mapping $\mathcal{T}_1^2$ which maps the state at liftoff of the 1. leg to the state at touchdown of the 2. leg, and an analogous map $\mathcal{T}_2^1$. Thus the return map reads $\mathcal{R} = \mathcal{T}_2^1 \circ r_2^1 \circ \mathcal{T}_1^2 \circ r_1^2$.

The dynamics of the LLS model can be described by four state variables $(v, \delta, \theta, \omega)$, where v is the center of mass speed, δ is the angle between the body axis and the mass center velocity vector, θ is the angle between the body axis and an inertial frame and $\omega = \dot{\theta}$. In [6] these four variables are augmented by two fixed parameters: β, the leg touchdown angle with respect to the body axis, and l_0, the relaxed leg length; and from the values of these six quantities at liftoff one can find the initial data for the next stance phase.

In these variables, the transition mapping $\mathcal{T}_1^2$ (omitting l_0) reads

$$\begin{aligned} \mathcal{T}_1^2 &\left((v_n^{LO} \ \delta_n^{LO} \ \theta_n^{LO} \ \omega_n^{LO} \ \beta_n^{LO})^\top\right) = \\ &(v_n^{LO} \ \delta_n^{LO} \ \theta_n^{LO} \ \omega_n^{LO} \ \beta)^\top \end{aligned} \quad (18)$$

where n stands for the nth stance phase, LO for liftoff, and β is held constant for all stance phases. If, as implicitly assumed for the SLIP treated above, β (and/or l_0) are regarded as state variables rather than parameters, then since they are 'reset' to fixed values at

---

[4]This is not true for approximations to the stance phase dynamics which violate the time reversing symmetry $\mathcal{S}_1$.

[5]Despite the fact that the determinant away from the fixed point is not 1 in this example, volume seems to be preserved in a finite region around the fixed point.
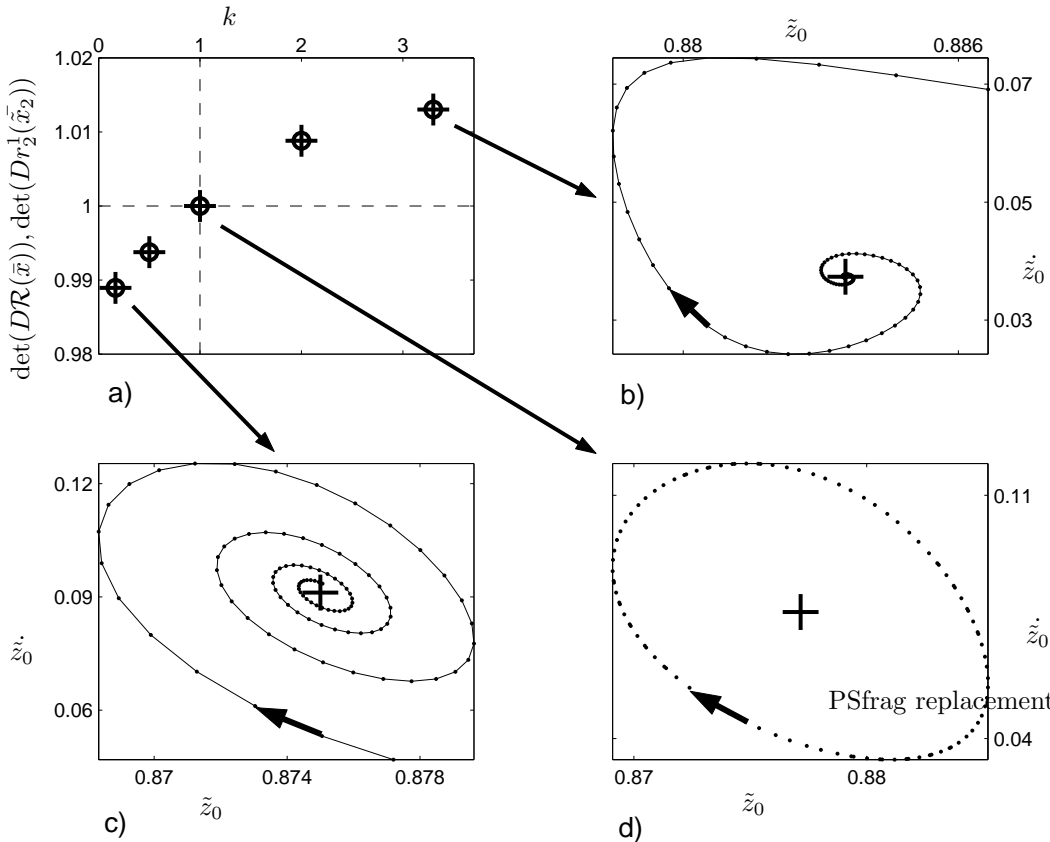
Figure 2: a) Comparison of the numerically computed determinant $\det(D\mathcal{R}(\bar{x}))$ (+) of the return map Jacobian to to the determinant $\det(Dr_2^1(\bar{\bar{x}}_2))$ (∘) obtained by using the numerically determined fixed points in eq. (17). b)-d) Trajectories around a fixed point. Because of the slow convergence, only every 9th iteration in plot b) and every 5th iteration in plot c) is shown.

touchdown, independent of their values at liftoff, the transition mapping $\mathcal{T}_1^2$ has rank four, volume is not preserved, and no deductions can be made regarding the reduced four-dimensional map. Restoring a nontrivial dynamical role to the variable β, for example, via a leg swing feedback strategy similar to (15), could lead to a non-degenerate mapping.

4   Conclusions

In this paper we used the example of the SLIP locomotion model to show how factored analysis of the return map may be a useful new tool in the stability analysis of hybrid Lagrangian systems. Specifically, we obtained a necessary condition for the asymptotic stability of SLIP in the presence of a leg recirculation strategy relevant to the operation of the robot RHex [1]. This condition is formulated in Sec. 3.1.3 for a particular family of leg recirculation strategies as an exact al-

gebraic expression despite the non-integrability of the SLIP system. Hence leg recirculation strategies that violate the above condition can be discarded without recourse to cumbersome numerical simulations. Application of this formalism to the robot RHex requires a more elaborate parametrization of leg recirculation schemes modeled after RHex's open loop controller.

This analysis can provide for the first time a partial explanation for the surprising self-stable behavior observed empirically in RHex. It also paves the way for a more principled investigation of detailed, biologically motivated leg placement strategies in the LLS model [6] which captures many aspects of cockroach locomotion [19].

Acknowledgements

Appendix: Invariance of the threshold equation for SLIP without pitching

In this appendix we show that the invariance of the threshold equation (11) under $S_2 \circ r_2^1 : \tilde{x}_{20} \mapsto S_2 \circ f_2^{\tilde{t}_{TD}}(\tilde{x}_{20})$ with $\tilde{x}_{20} = (\tilde{z}_0 \; \dot{\tilde{z}}_0)^\top$ corresponds to $|\det(Dr_2^1)| = 1$ for the leg recirculation family (15). First we observe that

$$f_2^{\tilde{t}}(\tilde{x}_{20}) = \begin{pmatrix} \tilde{z}_0 + \dot{\tilde{z}}_0 \tilde{t} - \frac{\tilde{t}^2}{2} \\ \dot{\tilde{z}}_0 - \tilde{t} \end{pmatrix} \quad (19)$$

$$S_2 \circ f_2^{\tilde{t}}(\tilde{x}_{20}) = \begin{pmatrix} \tilde{z}_0 + \dot{\tilde{z}}_0 \tilde{t} - \frac{\tilde{t}^2}{2} \\ -(\dot{\tilde{z}}_0 - \tilde{t}) \end{pmatrix} \quad (20)$$

$$f_2^{\tilde{t}} \circ S_2 \circ f_2^{\tilde{t}}(\tilde{x}_{20}) = \begin{pmatrix} \tilde{z}_0 \\ -\dot{\tilde{z}}_0 \end{pmatrix} \quad (21)$$

The threshold function $h_2^1(f_2^{\tilde{t}}(\tilde{x}_{20}), \tilde{x}_{20}, \tilde{t})$ becomes

$$h_2^1(f_2^{\tilde{t}}(\tilde{x}_{20}), \tilde{x}_{20}, \tilde{t}) = \tilde{z}(\tilde{t}) - \cos(\phi(\tilde{z}_0, \dot{\tilde{z}}_0, \tilde{t})) \quad (22)$$
with $\phi(\tilde{z}_0, \dot{\tilde{z}}_0, \tilde{t}) = k \arccos(\tilde{z}_0) + \alpha(\tilde{t} - l\dot{\tilde{z}}_0)$.

Then

$$h_2^1(f_2^{\tilde{t}_{TD}} \circ S_2 \circ f_2^{\tilde{t}_{TD}}(\tilde{x}_{20}), S_2 \circ f_2^{\tilde{t}_{TD}}(\tilde{x}_{20}), \tilde{t}_{TD}) = \quad (23)$$
$$\tilde{z}_0 - \cos\left(k \arccos(\tilde{z}_0 + \dot{\tilde{z}}_0 \tilde{t}_{TD} - \frac{\tilde{t}_{TD}^2}{2}) + \right.$$
$$\left. \alpha\left(\tilde{t}_{TD} + l(\dot{\tilde{z}}_0 - \tilde{t}_{TD})\right)\right) = 0$$

For a solution of this equation with the leg recirculating only once during flight $\phi(\tilde{z}_0, \dot{\tilde{z}}_0, \tilde{t}_{TD}) \in (\frac{3}{2}\pi, 2\pi)$. This must be taken into account when inverting the cosine:

$$\arccos(\tilde{z}_0) = -\left(k \arccos(\tilde{z}_0 + \dot{\tilde{z}}_0 \tilde{t}_{TD} - \frac{\tilde{t}_{TD}^2}{2}) + \right.$$
$$\left. \alpha\left(\tilde{t}_{TD} + l(\dot{\tilde{z}}_0 - \tilde{t}_{TD})\right)\right) + 2\pi$$
$$\Leftrightarrow \quad \cos\left(k \arccos\left(\tilde{z}(\tilde{t}_{TD})\right)\right) - \cos\left(\arccos(\tilde{z}_0) + \right.$$
$$\left. \alpha\left(\tilde{t}_{TD} + l(\dot{\tilde{z}}_0 - \tilde{t}_{TD})\right)\right) = 0$$
$$\overset{k=1, l=0}{\Leftrightarrow} \quad \tilde{z}(\tilde{t}_{TD}) - \cos\left(\arccos(\tilde{z}_0) + \alpha\left(\tilde{t}_{TD}\right)\right) = 0$$

For $k = 1$ and $l = 0$ this does reduce to the original threshold function (22) and we conclude that $|\det(Dr_2^1)| = 1$, as was explicitly derived in (17). For other values of k and l this does not in general reduce to (22), although we have not ruled out that for specific values of k and l and a specific form of α the original threshold function (22) is recovered.

References

[1] U. Saranli, M. Buehler, and D.E. Koditschek. Rhex: A simple and highly mobile hexapod robot. *The International Journal of Robotics Research*, 20(7):616–631, 2001.

[2] R. Altendorfer, N. Moore, H. Komsuoḡlu, M. Buehler, H.B. Brown Jr., D. McMordie, U. Saranli, R. Full, and D.E. Koditschek. Rhex: A biologically inspired hexapod runner. *Autonomous Robots*, 11:207–213, 2001.

[3] R. Blickhan and R. Full. Similarity in multilegged locomotion: Bouncing like a monopode. *J. Comp. Physiol.*, A(173):509–517, 1993.

[4] M.H. Raibert. *Legged Robots that Balance*. MIT Press, Cambridge, MA, 1986.

[5] T. Kubow and R. Full. The role of the mechanical system in control: a hypothesis of self-stabilization in hexapedal runners. *Philosophical Transactions of the Royal Society of London Series B - Biological Sciences*, 354(1385):849–861, 1999.

[6] J. Schmitt and P. Holmes. Mechanical models for insect locomotion: dynamics and stability in the horizontal plane I. Theory. *Biological Cybernetics*, 83:501–515, 2000.

[7] D.L. Jindrich and R. Full. Dynamic stabilization of rapid hexapedal locomotion. *Journal of Experimental Biology*, 205:2803–2823, 2002.

[8] A. Seyfarth, H. Geyer, M. Günther, and R. Blickhan. A movement criterion for running. *Journal of Biomechanics*, 35:649–655, 2002.

[9] R. M. Ghigliazza, R. Altendorfer, P. Holmes, and D. E. Koditschek. Passively stable conservative locomotion. submitted to *SIAM Journal of Applied Dynamical Systems*, 2002.

[10] A. Seyfarth, H. Geyer, R. Blickhan, and H. Herr. Does leg retraction simplify control in running? In *IV. World Congress of Biomechanics*, Calgary, Canada, 2002.

[11] R. Altendorfer. Passive stability of a clock-driven recirculating SLIP. unpublished.

[12] H.M. Herr and T.A. McMahon. A trotting horse model. *International Journal of Robotics Research*, 19 (6):566–581, 2000.

[13] P. Holmes. Poincaré, celestial mechanics, dynamical systems theory and "chaos". *Phys. Rep.*, 193(3):137–163, 1990.

[14] F. Scheck. *Mechanics: from Newton's laws to deterministic chaos.* Springer-Verlag, Berlin, 1999. Third edition.

[15] A. Ruina. Nonholonomic stability aspects of piecewise holonomic systems. *Reports on mathematical physics*, 42 (1-2):91–100, 1998.

[16] J. Guckenheimer and S. Johnson. Planar hybrid systems. In *Hybrid systems II: Lecture notes in computer science*, pages 202–225. Springer-Verlag, Berlin, 1995.

[17] M.J. Coleman and P. Holmes. Motions and stability of a piecewise holonomic system: the discrete Chaplygin sleigh. *Regular and chaotic dynamics*, 4(2):55–77, 1999.

[18] A. Ruina. The symmetry of some of the simple non-holonomic examples precludes asymptotic stability. Talk slides available at http://www.tam.cornell.edu/%7Eruina/hplab/ nonholonomics_papers.html.

[19] J. Schmitt, M. Garcia, R. Razo, P. Holmes, and R.J. Full. Dynamics and stability of legged locomotion in the horizontal plane: A test case using insects. *Biological Cybernetics*, 86 (5):343–353, 2002.